

Utilization of X-ray diffraction data in machine-learning based material exploration for all-solid-state lithium batteries

Kota Suzuki*, Masaaki Hirayama*, and Ryoji Kanno*,**

1. Introduction

Lithium-ion batteries are secondary (rechargeable) batteries that are used for a wide range of applications, from mobile devices to electric vehicles, as they combine both high energy density and excellent power characteristics. In recent years, research has been conducted toward the realization of an all-solid-state lithium battery, in which the organic electrolyte is replaced with a solid lithium conductor (Fig. 1). In many existing battery systems, including lithium-ion batteries, the electrolyte in which the supporting salt is dissolved is responsible for transporting carrier ions between the electrodes; in all-solid-state batteries, ion transport is performed by a solid electrolyte. At the same time, electrons flow through the external circuit, delivering power to the devices. The use of a solid electrolyte is believed to eliminate problems such as liquid leakage and electrical shorts, as well as explosions that can occur when an organic electrolyte is used, thus improving safety and reliability.

Discovering and producing an effective solid electrolyte is a significant challenge in developing solid-state lithium batteries. This means that a pure ionic conductor is required, in which only lithium ions diffuse at high speed, without electron conduction taking place. Various material systems, such as glass, glass ceramics, crystals, and polymers, have been developed as solid electrolytes^{(1),(2)}. Thus far, sulfide-based materials are the only materials that exhibit ionic conductivity characteristics comparable to existing liquid electrolytes ($\geq 10^{-2} \text{ S cm}^{-1}$)⁽³⁾⁻⁽⁵⁾.

Many researchers have been developing and analyzing potential electrode materials and solid electrolytes, with a particular focus on crystalline materials. All-solid-state lithium batteries would give rise to the possibility of all battery components being made from crystalline materials; therefore, the importance of phase identification and crystal structure analyses by X-ray diffraction (XRD) measurements will increase.

In this technical note, we will introduce XRD measurements and explore how the data can be used in the search for materials related to all-solid-state batteries, along with examples of our own research.

2. Introduction of a Case Study of Material Search Using Machine Learning

To realize all-solid-state lithium batteries, solid electrolyte materials that exhibit lithium conductivity are being developed. Sulfide-based materials with high ionic conductivity are the primary focus, but there is also interest in the development of oxide-based materials that are highly stable. Synthesis conditions and compositional optimization are at the core of the development of oxide systems based on existing crystalline materials that have relatively high conductivity at room temperature ($\sim 10^{-3} \text{ S cm}^{-1}$), such as lithium superionic conductors (LISICON), perovskite, and garnet crystals. Meanwhile, in 2018, LiTa_2PO_8 ($1.6 \times 10^{-3} \text{ S cm}^{-1}$), a new material with a unique composition and crystal structure, was reported⁽⁶⁾, suggesting the possibility of discovering materials of

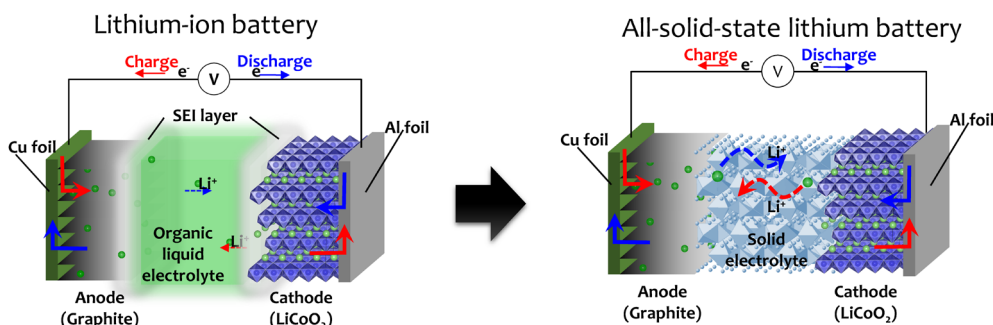


Fig. 1. Schematic diagram of constituent materials and reactions of lithium-ion and all-solid-state lithium batteries.

* School of Materials and Chemical Technology, Tokyo Institute of Technology.

** Institute of Innovative Research, Tokyo Institute of Technology.

Phase diagram selection: Li-Zn-Ge-O

→ LISICON-based Li conductor

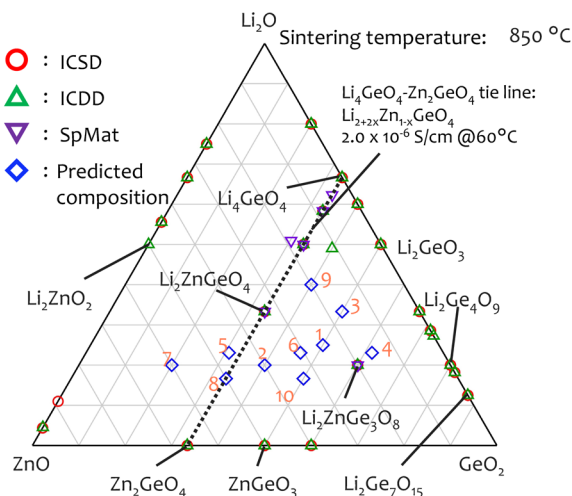
P.G. Bruce, A.R. West, *Mater. Res. Bull.*, 15, 379-385 (1980).

Fig. 2. Example of a material search utilizing the recommender system and Li-Zn-Ge-O composition: synthesis and evaluation are performed while referring to a map, which is a pseudo-ternary phase diagram containing reported materials and predicted compositions.

novel composition and structure in the search for a feasible oxide electrolyte. However, searching for materials with unexplored compositions requires a lot of labor, and success relies strongly on the experience and intuition of the researchers. Therefore, there is a need to develop a highly efficient approach to search for materials that shortens the process leading to material discovery.

We have been working with Dr. Isao Tanaka and Dr. Atsuto Seko of Kyoto University to develop an efficient way to search for new materials using machine-learning techniques. We focused on the development of new material search methods by combining unknown stable composition prediction using recommendation systems^{(7), (8)} and synthetic chemistry (element selection). The aim is to efficiently find new oxide-based materials that exhibit excellent lithium-ion conductivity. Recommender systems are commonly employed to recommend unpurchased products to users that suit their interests and tastes using their internet purchase and browsing histories, and is one of the most common machine learning methods available. When such a recommender system is applied to material development, the chemical compositions contained in a database of known materials, such as ICSD, are used as learning data to propose unknown compositions with a high possibility of existence. For example, by learning the known combinations of M , M' , a , b , c , and d , denoted $\text{Li}_a\text{M}_b\text{M}'_c\text{O}_d$, it is possible to predict (recommend) an unreported combination of elements and composition ratios based on the degree of similarity. Since the predicted composition contains information (expected value) related to the probability of existence, a relative expected value can be obtained for the

Table 1. Li-Zn-Ge-O compositions predicted from the recommender system.

No.	Predicted composition	Indicator of stability
1	$\text{Li}_2\text{ZnGe}_2\text{O}_6$	0.1467
2	$\text{Li}_2\text{Zn}_2\text{Ge}_2\text{O}_7$	0.0914
3	$\text{Li}_4\text{ZnGe}_3\text{O}_9$	0.0156
4	$\text{Li}_6\text{Zn}_2\text{Ge}_8\text{O}_{21}$	0.0135
5	$\text{Li}_6\text{Zn}_6\text{Ge}_4\text{O}_{17}$	0.0099
6	$\text{Li}_6\text{Zn}_4\text{Ge}_6\text{O}_{19}$	0.0095
7	$\text{Li}_2\text{Zn}_3\text{Ge}_6\text{O}_6$	0.0093
8	$\text{Li}_2\text{Zn}_3\text{Ge}_2\text{O}_8$	0.0092
9	$\text{Li}_4\text{ZnGe}_2\text{O}_7$	0.0086
10	$\text{Li}_2\text{Zn}_2\text{Ge}_3\text{O}_9$	0.0077

possibility of existence of the material. This can be more easily understood by thinking of the process as being equivalent to a product of high similarity or relevance to a previously purchased product showing up in a “recommended product” section while browsing. In other words, information regarding the chemical composition database recommended by machine learning provides important guidance in determining a specific search area (chemical composition) for finding a new material after selecting an element combination.

We will now explain the process of material search. First, it is necessary to select constituent elements that are expected to have high ionic conductivity; in this example, we focused on the phase diagram of Li-Zn-Ge-O^{(11), (12)} in which LISICON was reported^{(9), (10)}. A pseudo-ternary phase diagram of $\text{Li}_2\text{O-ZnO-GeO}_2$ is created, as shown in Fig. 2, and reported materials are plotted. There is a classical technique that involves synthesizing solid solutions by searching on the tie line of known materials, which requires exhaustively selecting and synthesizing compositions. In this situation, the probability that an unknown material with a new composition exists is only a prediction based on the researcher’s knowledge, experience, and intuition, and it is unlikely that a new material will be found. By making good use of a recommender system in such situations, it is possible to identify compositions that are likely to form a stable phase. Unknown chemical compositions predicted by the recommender system are shown in Table 1 and are plotted in Fig. 2. The points represented by diamonds in the figure are the compositions predicted by the recommender system, and the numbers shown next to them correspond to the rank of probability of existence in the phase diagram. From here, promising search areas and compositions will be determined specifically, before carrying out synthesis and evaluation. Based on these guidelines, we have found novel lithium conductors in Li-Ge-P-O systems, Li-Zn-Ge-O systems, etc.

Here, we introduce the XRD patterns obtained while searching through the pseudo-ternary phase diagram (Fig. 3). Measurements were taken using SmartLab (Rigaku, $\text{Cu K}\alpha$) with a 2θ scanning range of $10\text{--}50^\circ$ and a step width of 0.01° . The phases in the XRD patterns

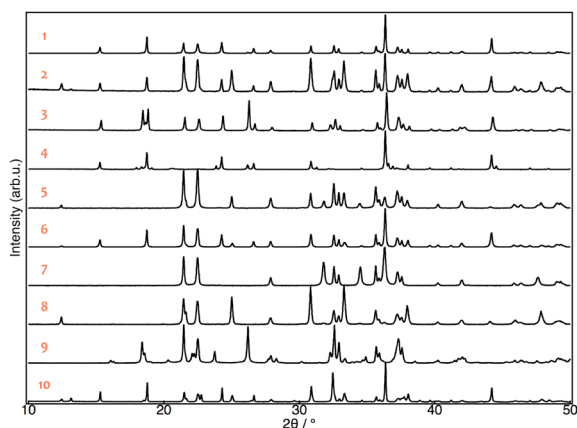


Fig. 3. XRD patterns of the Li–Zn–Ge–O system materials obtained by material search.

were identified using PDXL (Rigaku), and the crystal phases obtained from each composition were assigned to known and unknown phases, which are summarized in Table 2. It was found that unknown phases (Unknown I, II) were obtained when the samples were synthesized according to the ratios of predicted compositions 4 and 10, respectively. On the other hand, when synthesized using other compositional ratios, we obtained a mixed phase of known materials. The known materials detected were mainly starting materials, lithium-free composite oxides, or LISICON-related phases. To create a new material, we focused on the unknown phases. Predicted composition 4 was chosen in particular as it contains Unknown I, which is thought to have a higher Li content than Unknown II.

In Predicted Composition 4 ($\text{Li}_6\text{Ge}_8\text{Zn}_2\text{O}_{21}$), we confirmed both known (Li_2GeO_3 and $\text{Li}_2\text{ZnGe}_3\text{O}_8$) and unknown (Unknown I) phases. Despite fixing the preparation ratio of the main materials to that of the predicted composition and examining the treatment conditions of the precursor (e.g., calcination temperature and time, etc.), it was difficult to reduce the number of impurities. Therefore, we believed that the composition of Unknown I was significantly different from Predicted Composition 4 and tried to estimate it.

The composition ratio of known materials was estimated from the intensity ratio of the diffraction lines using PDXL, and it was found to be $\text{Li}_2\text{GeO}_3:\text{Li}_2\text{ZnGe}_3\text{O}_8 = 23:77$. The net composition of all impurities was calculated based on this information. Considering that the unknown phase existed in the region of the extension line connecting this net composition and the preparation composition ($\text{Li}_6\text{Zn}_2\text{Ge}_8\text{O}_{21}$), synthesis and phase identification were carried out by expanding the search area (Fig. 4). It was found that Unknown I could be synthesized almost entirely of monophasic $\text{Li}_3\text{Zn}_{0.65}\text{Ge}_{4.35}\text{O}_{10.85}$. As seen in the XRD results in Fig. 4, under optimized composition and synthesis conditions, the diffraction peaks attributed to Li_2GeO_3 and $\text{Li}_2\text{ZnGe}_3\text{O}_8$ largely disappeared. In addition, scanning electron microscopy (SEM)/energy-dispersive X-ray spectroscopy (EDX) observations

Table 2. Phase identification results of Li–Zn–Ge–O samples obtained by material search.

No.	Predicted composition	Phases identified
1	$\text{Li}_2\text{ZnGe}_2\text{O}_6$	$\text{Li}_2\text{ZnGeO}_4$ $\text{Li}_2\text{ZnGe}_3\text{O}_8$
2	$\text{Li}_2\text{Zn}_2\text{Ge}_2\text{O}_7$	$\text{Li}_2\text{ZnGeO}_4$ $\text{Li}_2\text{ZnGe}_3\text{O}_8$ Zn_2GeO_4
3	$\text{Li}_4\text{ZnGe}_3\text{O}_9$	$\text{Li}_2\text{ZnGeO}_4$ $\text{Li}_2\text{ZnGe}_3\text{O}_8$ Li_2GeO_3
4	$\text{Li}_6\text{Zn}_2\text{Ge}_8\text{O}_{21}$	Unknown I $\text{Li}_2\text{ZnGe}_3\text{O}_8$ Li_2GeO_3
5	$\text{Li}_6\text{Zn}_6\text{Ge}_4\text{O}_{17}$	$\text{Li}_2\text{ZnGeO}_4$ Zn_2GeO_4 ZnO
6	$\text{Li}_6\text{Zn}_4\text{Ge}_6\text{O}_{19}$	$\text{Li}_2\text{ZnGeO}_4$ $\text{Li}_2\text{ZnGe}_3\text{O}_8$ Zn_2GeO_4
7	$\text{Li}_2\text{Zn}_3\text{GeO}_6$	$\text{Li}_2\text{ZnGeO}_4$ ZnO
8	$\text{Li}_2\text{Zn}_3\text{Ge}_2\text{O}_8$	$\text{Li}_2\text{ZnGeO}_4$ Zn_2GeO_4 ZnO
9	$\text{Li}_4\text{ZnGe}_2\text{O}_7$	LISICON $\text{Li}_2\text{ZnGeO}_4$ Li_2GeO_3
10	$\text{Li}_2\text{Zn}_2\text{Ge}_3\text{O}_9$	Unknown II $\text{Li}_2\text{ZnGeO}_4$ $\text{Li}_2\text{ZnGe}_3\text{O}_8$ Zn_2GeO_4 Li_2O

confirmed that the synthesized sample showed an almost uniform elemental distribution, confirming that a new material with a novel composition and an unknown structure was obtained.

The ionic conductivity of this new material was evaluated by the AC impedance method (Fig. 5). The ionic conductivity of a cold-pressed pellet sample at room temperature, including the bulk and grain boundaries, was $2.2 \times 10^{-7} \text{ S cm}^{-1}$, and its activation energy was determined to be 40 kJ mol^{-1} . To separate the bulk and grain boundary components, the ionic conductivity of the sample was evaluated after re-calcination. Although it was difficult to separate the resistance components under the conditions examined, the resistance—including bulk and grain boundaries—decreased, and its ionic conductivity was $1.1 \times 10^{-6} \text{ S cm}^{-1}$ at room temperature. By looking at the XRD data before and after re-calcination, we saw that diffraction peaks sharpened, and crystallinity improved. Furthermore, we found that the relative density of the pellets increased by approximately 18% from synthesis

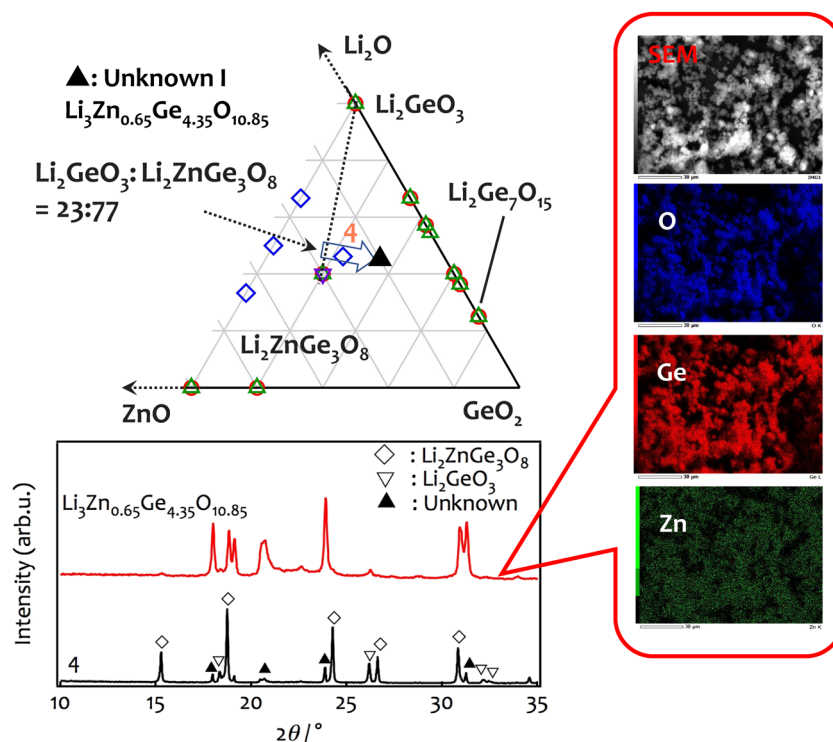


Fig. 4. Material search procedure around Predicted Composition 4 ($\text{Li}_6\text{Ge}_8\text{Zn}_2\text{O}_{21}$), XRD patterns and results of SEM/EDX observations of the optimized composition.

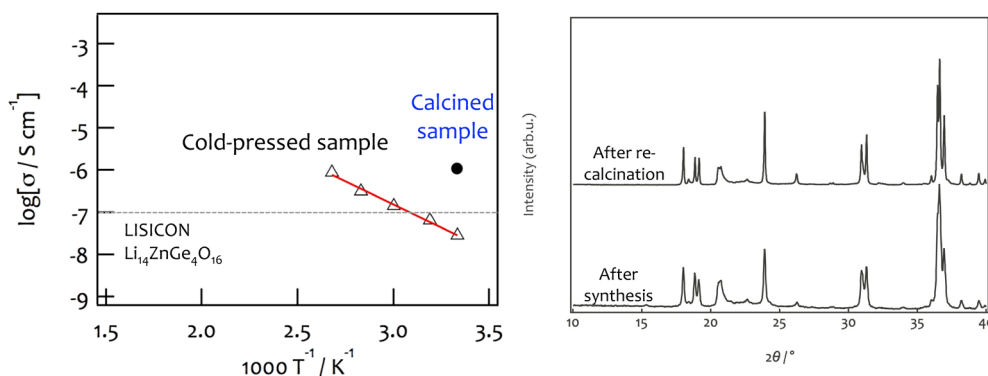


Fig. 5. Ionic conductivity and XRD patterns of $\text{Li}_3\text{Zn}_{0.65}\text{Ge}_{4.35}\text{O}_{10.85}$ before and after re-calcination.

(2.62 g cm^{-3}) to re-calcination (3.08 g cm^{-3}). It was revealed that the improvement in ionic conductivity was influenced by the decrease in the resistance components of the bulk and grain boundaries. In addition, the ionic conductivity after re-calcination reached about twice that of $\text{Li}_{14}\text{Zn}(\text{GeO}_4)_4$ ⁽¹⁰⁾, which has a similar composition, and a relatively high conductivity among LISICON-based materials. A lithium conductor ($\text{Li}_6\text{Ge}_2\text{P}_4\text{O}_{17}$) with a new composition and unknown structure was found in the Li–Ge–P–O system using a recommender system, XRD measurements, phase identification, and data interpretation. Until now, we have not discovered a superionic conductor that can be used as a flagship material. However, by combining machine learning and synthetic chemistry methods and ideas, we can expect to streamline the search for ionic conductors. In addition, by elucidating the crystal

structures of unknown phases found through a series of studies, it will be possible to start a material search using new materials.

3. Conclusion

In this technical note, we introduced the role of XRD measurement and diffraction data in the search for new materials. As an example, we chose to explore all-solid-state lithium battery-related materials, especially solid electrolytes. As previously mentioned, XRD analysis is one of the most powerful methods for the search and evaluation of materials suitable for solid electrolytes. This is the latest approach to material search that utilizes machine learning, but the acquisition and interpretation of diffraction data are based on classical methods and ideas. Of course, at the cutting-edge, high-speed measurements using automatic sample exchangers

and two-dimensional detectors and the deployment of computational methods that combine data analysis and clustering analysis by automatic peak search are also progressing. In other words, it has become possible to incorporate combinatorial and machine learning methods into the determination of material search guidelines, data acquisition, and analysis. At the same time, there is currently no one-size-fits-all method that makes everything possible. The most important aspect of modern material searches should be to combine the established and highly reliable classical search methods, experiments, and analytical techniques with the latest combinatorial experiments and computational methods to improve the search efficiency of a target material or material system.

References

- (1) Y. Kato, S. Hori and R. Kanno: *Adv. Ener. Mater.*, **10** (2020), 2002153.
- (2) Q. Zhao, S. Stalin, C.-Z. Zhao and L. A. Archer: *Nat. Rev. Mater.*, **5** (2020), 229–252.
- (3) Y. Kato, S. Hori, T. Saito, K. Suzuki, M. Hirayama, A. Mitsui, M. Yonemura, H. Iba and R. Kanno: *Nature Energy*, **1** (2016), 16030.
- (4) Y. Seino, T. Ota, K. Takada, A. Hayashi and M. Tatsumisago: *Energy Environ. Sci.*, **7** (2014) 627–631.
- (5) M. A. Kraft, S. Ohno, T. Zinkevich, R. Koerver, S. P. Culver, T. Fuchs, A. Senyshyn, S. Indris, B. J. Morgan and W. G. Zeier: *J. Am. Chem. Soc.*, **140** (2018), 16330–16339.
- (6) J. Kim, J. Kim, M. Avdeev, H. Yun and S.-J. Kim: *J. Mater. Chem. A*, **6** (2018), 22478–22482.
- (7) A. Seko, H. Hayashi, H. Kashima and I. Tanaka: *Phys. Rev. Materials*, **2** (2018), 013805.
- (8) A. Seko, H. Hayashi and I. Tanaka: *J. Chem. Phys.*, **148** (2018), 241719.
- (9) P. G. Bruce and A. R. West: *Mater. Res. Bull.*, **15** (1980), 379–385.
- (10) U. v. Alpen, M. F. Bell, W. Wichelhaus, K. Y. Cheung and G. J. Dudley: *Electrochim. Acta*, **23** (1978), 1395–1397.
- (11) K. Suzuki, K. Ohura, A. Seko, Y. Iwamizu, G. Zhao, M. Hirayama, I. Tanaka and R. Kanno: *J. Mater. Chem. A*, **8** (2020), 11582–11588.
- (12) K. Suzuki and R. Kanno: *Denki Kagaku (Electrochemistry)*, **88** (2020), 3–8. [in Japanese]